Edge and particle embedment effects in low- and high-stress slurry erosion wear of steels and elastomers

N. Ojala[1]*, K. Valtonen[1], J. Minkkinen[2] and V.-T. Kuokkala[1]

[1]*Tampere University of Technology, Laboratory of Materials Science, Tampere Wear Center, P.O.Box 589, FI-33101 Tampere, Finland*
[2]*SSAB Europe Oy, FI-13100 Hämeenlinna, Finland*

Abstract

Slurry transportation via pumping is an increasingly viable alternative for the conventional fine particle pumping, but there are also many applications involving larger particles. However, most of the published studies on slurry erosion have been conducted with fine particle sizes. In this work, also large particle slurry erosion of commercial wear resistant materials is studied. A high speed slurry-pot wear tester was used with edge protected samples to simulate the wear conditions in industrial slurry applications where edge wear is minimal. Two wear resistant steels together with natural rubber and polyurethane lining materials were tested, and the results were compared with the results of the same materials tested without sample edge protection. The tests were performed using 15 m/s speed, two sample angles, and slurry concentrations with particle size ranging from large 8/10 mm granite to fine 0.1/0.6 mm quartz. In all conditions, the steel samples showed stable wear behavior, whereas the elastomers gave notably inconsistent results in different test conditions. In general, steels exhibited better wear performance with large particles and elastomers with fine particles, and the wear losses were 40-95 % lower when edge wear was inhibited. With increasing abrasive size, the edge wear becomes more dominant and the particle embedment decreases.

Keywords: Wear testing; Steel; Elastomers; Edge effect; Particle embedment; Mining, mineral processing

*Corresponding author: Niko Ojala (niko.ojala@tut.fi)

1. INTRODUCTION

Slurry pumping is a sustainable option for transporting solids in large mining related operations. The slurry pipeline technology is relatively young with about 10,000 kilometers of active pipeline around the world. For the first time, minerals were transported via a pipeline in the 1960's, whereas long distance pipelines, i.e., longer than about 900 km, emerged only in the 1990's. [1] At the same time, slurry transport has replaced conveyors in mines [2]. In general, slurry is defined as a mixture of liquid and solid particles that can be transported by pumping [3]. Particle size and also the speed of the slurry can vary quite widely from application to application [4–6]. The particle size can be from fine micron size particles to large particles of tens of millimeters in size [3]. In the published studies, larger particle sizes have not been extensively used. Mostly the particles used in slurry wear experiments have been under one millimeter in size [7–9]. Large particle sizes have only been used by Jankovic [10] (up to 5 mm particles) and Ojala et al. [5,6,11] (same 8-10 mm particles

as in this study). In soil abrasion tests with a pot tester, Jakobsen [12] have used up to 10 mm particles with high 75 – 100 % concentration of solids.

The industrial slurry applications related to mining can be divided into two categories, small and large particle applications [6]. In the small particle applications, normally particles smaller than 1 mm in size are handled with slurry concentrations typically between 50 and 70 wt% and slurry flow speeds varying in the range of 10-25 m/s [4]. In the large particle applications, the particle size can be up to 50 mm with concentrations typically lower than with small particles at around 10-20 wt%, and with speeds up to 30 m/s [13]. In addition, especially with large particles as for example in dredging, the concentration and particle size may fluctuate quite much during the operation. As an application oriented wear tester, the high speed slurry-pot has highly turbulent wear conditions inside the pot, which correlates quite well with many practical applications. The test method generates a wide distribution of particle impact angles but still provides a good working environment and reproducible test results [5].

Only a few of the slurry erosion related publications deal with quenched steels [14–16] or elastomers [17]. Madsen [18], who tested both quenched steels and elastomers compared several steels and a couple of elastomers using both laboratory-prepared slurries and slurries acquired from the field. In the tests, he used a laboratory tester with edge protected samples. He concluded that with the 2 wt% 0.2/0.3 mm laboratory sand slurry the elastomers had an advantage over the tested metals, but with the field slurries with abrasive size up to 1.7 mm, white cast iron and wear resistant steels were better or on par with the elastomers. Also Xie et al. [19] compared steels and elastomers using fine particles with three different low-stress slurry wear test devices. In the tests with two of these devices, the samples were edge protected. Xie et al. concluded that during slurry transportation the impact angles of the particles are random, i.e., the flow is turbulent. In their fine particle low-stress slurry tests, elastomers had supreme wear resistance over the steels.

In the studies published on slurry wear [14–16,18–26], five different wear tester types have been used: a Coriolis erosion tester, slurry-jets, a pilot pipe circuit, slurry-pots, and slurry sliding abrasion tester. All of these systems have been, or could have been, equipped with edge protected samples, but none of the studies addressed the effect of edge wear or its influence on the wear process.

Edge wear and its effect on overall wear losses have been studied before in dry conditions. Terva et al. [27] studied edge wear in high-stress abrasion with different-sized granite and quartz abrasives using structural and tool steels. They concluded that the edge effect may vary between 1 – 50 %, depending on the abrasive size and type and the tested material. With granite the edge effect was bigger than with quartz. The largest abrasive size used, i.e., 8/10 mm, caused the highest edge wear for both materials. Ratia et al. [28] studied the role of edge-concentrated wear in high-stress impact-abrasion with large granite abrasives at two different sample angles using two structural steels and a 400HB wear resistant steel. They concluded that the edge effect varied

between 80 – 97 % in 45 minute tests and between 66 – 82 % in 270 minute tests, depending on the sample angle. A larger sample angle caused a stronger edge effect.

In a previous [6] study, marked differences in particle embedment were observed between steels and elastomers, but also between different abrasives. For the steels, the embedment was only sticking of individual abrasives on the steel surface or occasional tribolayer formation by mixing of the two materials. For elastomers, however, a much stronger embedding tendency was observed with X-ray computer tomography, which revealed that although the particles penetrated only the very surface of the material, the particle concentration on the surface was high.

After the pioneering work of Hutchings [29] on particles deforming ductile materials, particle embedment has been studied in numerous studies [30–39]. In recent years, these studies have been much focused on numerical modeling, such as the work by Hadavi et al. [40]. The published results about the particle size effect have shown differences between metals and elastomer. For example, Getu et al. [38] reported that the particle size had no effect with the tested polymer materials, while for example Hadavi et al. [39] reported that embedment increases with the particle size in the case of aluminum. In these studies, Getu et al. used particles below the size of 200 µm, and Hadavi et al. below the size of 300 µm. Lathabai et al. [32] and Getu et al. [37] observed that with particles below the size of 700 µm and polymer materials, the embedded particles can protect the surface and reduce the wear rate. About the influence of larger particles, no information is available other than the observations done by Ojala et al. with steels and elastomers in the previous study [6]. In particular, the influence of the embedment on the ranking of different materials has not been studied before.

In demanding slurry applications, the abrasive wear mechanism dominates, as the abrasivity of the slurry is usually high because of the high slurry flow speeds and/or large particles inside the slurry. This wear type is generally called abrasive slurry erosion [6,41], where also corrosion is less significant [20,42]. In this work, the high speed slurry-pot wear tester was used with edge protected samples to simulate the wear conditions in industrial slurry applications where edge wear is limited or nonexistent, such as tanks and pipelines. The test materials included two wear resistant steels and two elastomers. The same materials were tested in the previous work [6] without edge protection, and therefore the edge effect could be evaluated by comparing the results of these two studies. The edge effect was studied with both fine and large particles. The wear performance of the materials was evaluated based on the wear tests and wear surface characterizations.

2. MATERIALS AND METHODS

The test parameters were set to simulate the demanding conditions in slurry pipelines. The test device was the high speed slurry-pot wear tester [5] at the Tampere Wear Center. The test materials, presented in Table 1, included two wear resistant steels with hardness grades of 400 and 500 HB, and two wear resistant elastomers, i.e., a natural rubber and a polyurethane. All materials are commercially available. In the table the hardness

values of the steels were measured, while the other values are typical values reported by the manufacturers. The nominal alloying of the steels was similar, but there were small differences in their microstructure. Both steels had an auto-tempered martensitic microstructure. The grain size of the 400HB steel was smaller than that of the 500HB steel. Small white areas seen in Fig. 1 are untempered (white) martensite.

Table 1: *Test materials.*

Steels	400HB	500HB	**Elastomers**	NR	PU
Hardness [HV10]	414 ± 4	554 ± 2	Hardness [ShA]	40	75
Yield strength [N/mm^2]	1000	1250	Tensile strength [N/mm2]	25	23
Tensile strength [N/mm2]	1250	1600	Density [g/cm^3]	1.04	1.05
A5 [%]	10	8	Isocyanate type	-	MDI
Density [g/cm^3]	7.85	7.85	Polyol type	-	polyether
C [max%]	0.23	0.3			
Si [max%]	0.8	0.8			
Mn [max%]	1.7	1.7			
P [max%]	0.025	0.025			
S [max%]	0.015	0.015			
Cr [max%]	1.5	1			
Ni [max%]	1	1			
Mo [max%]	0.5	0.5			
B [max%]	0.005	0.005			

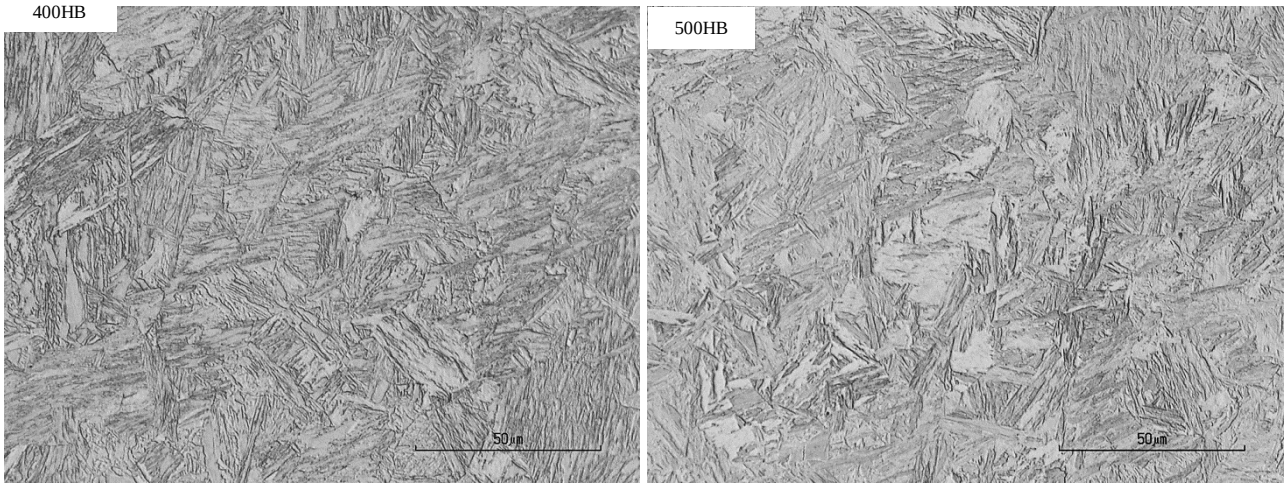

Figure 1: *Optical micrographs of the studied steels.*

The steel samples were 6 mm thick and the elastomer samples 5 mm thick. Otherwise all samples were 35 x 35 mm square plates. Edge protection was done with window plates having a 33 x 33 mm opening. 1 mm thick shim plates were placed under the elastomer samples to assure tight fitting inside the sample holder. The test setup was the same as used in the previous study [6] with unprotected plate samples. The wear tester is a pin mill type slurry-pot, where the samples are attached to a vertical rotating main shaft in horizontal positions at

different height levels. Two lowermost sample levels and two sample angles, 45° and 90°, were used in these tests, as presented in Fig. 2.

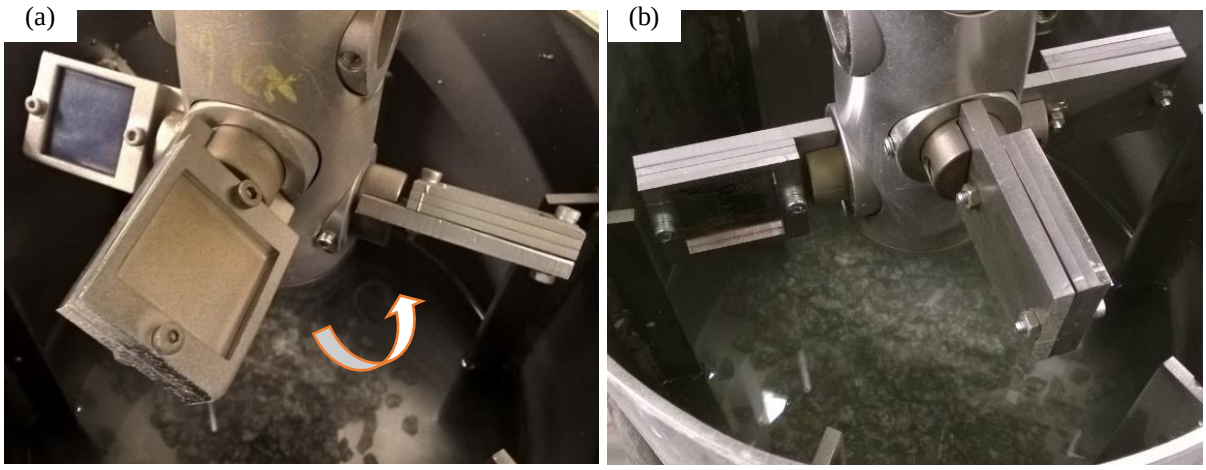

Figure 2: *Sample arrangements with a) +45° (the arrow indicates the direction of shaft rotation) and b) 90° sample angles*

The test preparations were as follows: the samples were first attached to the sample holders, the shaft was lowered into the pot, and the slurry was added. After that the samples were spun at 1500 rpm in the pot. The test time was first 20 minutes, after which the test was continued for another 60 minutes. Every test, lasting 20 or 60 minutes, consisted of four 5 or 15 minute cycles. The sample rotation test method [5] was utilized, in which the sample positions are switched and the slurry is renewed after every cycle. Sample rotation assures that all samples have experienced similar conditions when the test is completed. Moreover, it minimizes the scatter in the results caused by the possible differences in the test conditions between the different sample positions. After the tests, the wear rates were determined by weighing and the volume losses were calculated using material densities. Comminution of the abrasives was evaluated by sieving the used abrasives after the tests.

Table 2 presents the test parameters selected on the basis of the previous study [6]. The largest and the finest abrasives used in the previous study were selected also for the present study, but the actual sample tip speed decreased by 1 m/s due to the use of the edge protecting window. The shaft speed was kept at the same value of 1500 rpm as before for not to change the comminution of the abrasives and the slurry flow characteristics more than caused by the slightly different sample holder. As an addition to the previous study, the fine quartz slurry tests were conducted also with the 90° sample angle. The focus of the tests, however, was on the 45° sample angle, and therefore the continuation tests were conducted only with it. Similarly, repetitions were done only for the 45° tests, where 2…3 samples of each material were tested. The average standard deviation of all results with edge protection is only 3 %. The slurry concentration was 9 wt% with large granite abrasives, because the edge protection windows did not endure higher slurry concentrations sufficiently. The granite gravel with hardness of 800 HV1 was from Sorila quarry in Finland. The quartz sand with hardness of 1200 HV1, in turn, was from Nilsiä quarry in Finland. The density of both abrasives was 2.6 g/cm^3 [43]. To analyze

the comminution of the abrasives, they were collected after each test and sieved using mesh sizes from 0.036 to 10 mm.

Table 2: *Test parameters used in the tests.*

Abrasive	Particle size [mm]	Sample tip speed [m/s]	Slurry concentration [wt%]	Sample angle [°]	Test time [min]
Granite	8/10	14	9	90	4 x 5
				+45	4 x 5 + 4 x 15
Quartz	0.1/0.6		33	90	4 x 5

All samples were water jet cut, and the surfaces of the steel samples were ground to remove the possible decarburization layers. Vickers hardness (HV10) of the steel sample surfaces were measured before the tests diagonally over the test surfaces. The wear surfaces of all samples were analyzed with optical 3D-profilometer (Alicona InfiniteFocus G5), and the steel samples also with a scanning electron microscope (SEM, Philips XL 30). The cross-sections of the steel samples were analyzed with SEM, and the microhardness values were measured with a microhardness tester (HV50gf). Nital was used for etching of the cross-section samples.

3. RESULTS

Fig. 3 presents the wear test results for the 4 x 5 minute tests at both sample angles. For the steels the order is clear: the harder of the two steels is more wear resistant in all conditions. The difference between the steels is largest with the fine abrasive size, being 45 % at the 45° sample angle with fine quartz slurry but only 20 % with large granite slurry, irrespective of the slurry concentration. At the 90° sample angle the difference with fine particles is as high as 75 %. The larger test angle causes more wear in the steels, while the opposite is true for the natural rubber, especially with large particles. At the 90° sample angle the steels showed the highest volume losses, reducing to about half when the sample angle was decreased to 45°. The natural rubber, instead, shows lower volume losses at the 90° sample angle, which with large particles is doubled when the sample angle is changed to 45°. Polyurethane, on the other hand, shows a huge difference between the two slurries at the 90° angle but quite a small difference at 45°. In 20 (4 x 5) minute tests the natural rubber has the best overall wear resistance at the 90° sample angle, polyurethane being even better with the fine particles. At the 45° sample angle the 500HB steel showed the best wear performance with large particles and the natural rubber with fine particles. The behavior of the polyurethane samples was somewhat inconsistent, showing more wear with large particles at the high angle but the opposite with fine particles. This obviously is a result of the rather high hardness of the polyurethane.

A rather striking feature in the results is that the smaller abrasive size causes larger volume losses in the steels and also in the polyurethane at the 45° sample angle. It should, however, be noted that the slurry concentration

was higher (33 %) with the fine particles. The 33 wt% 8/10 mm granite slurry was also used in the tests with the 45° sample angle, but it was too aggressive for the sample holder setup for completing the test program. However, the results indicate that the difference to the fine quartz slurry in the wear rate was about twofold for the steels and up to 30 times for the elastomers.

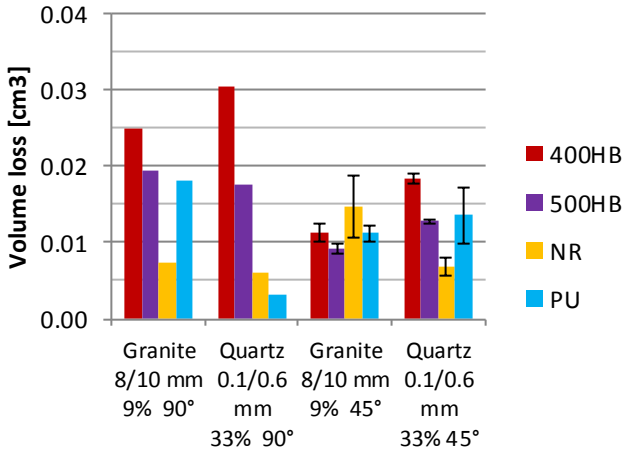

Figure 3: *Results of the 4 x 5 minute wear tests.*

For the 45° sample angle, also continuation tests were done for evaluating the progress of the slurry erosion process in the test materials. Fig. 4 presents the full set of results, including both the 20 and 60 minute test parts. With the large particle granite slurry, the progress is rather linear, natural rubber showing some change towards smaller volume losses. With the fine particle quartz slurry, the 400HB steel continues to wear quite linearly, while the other materials exhibit a slightly decreasing wear rate with increasing test time. The scatter in the volume loss values of the steels was very small, 0.4 – 4.8 %, so that their error bars are not visible behind the data points in the figure.

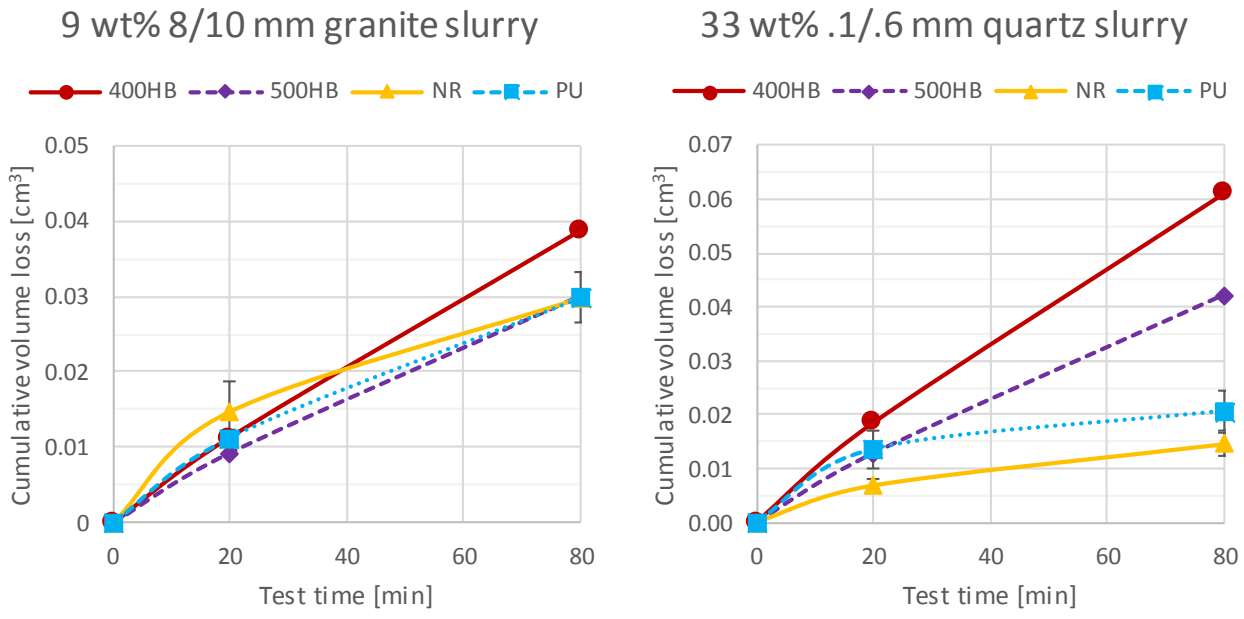

Figure 4: *Wear test results of all samples tested with the 45° sample angle.*

3.1. Comminution of the abrasives

Abrasives were collected after each test and sieved to analyze the degree of comminution. Fig. 5 presents the data for both abrasives used in this study, and Fig. 6 shows a picture of unused and used abrasives. It is notable that the initially large granite abrasives are strongly comminuted during the tests, but nothing much has happened to the already initially fine quartz particles. As could be expected, the longer the test time, the more granite is comminuted: in the 20 minute tests, i.e., with 5 minute test cycles, 50 % of the particles still remain larger than 4 mm in average size, while in the 60 minute tests, i.e., with 15 minute test cycles, the corresponding value is only 22 %. Although the comminution is high with granite abrasives, it does not affect the appearance of the mass loss plots, as the effect is averaged out by the renewal of the slurry batch after every test cycle.

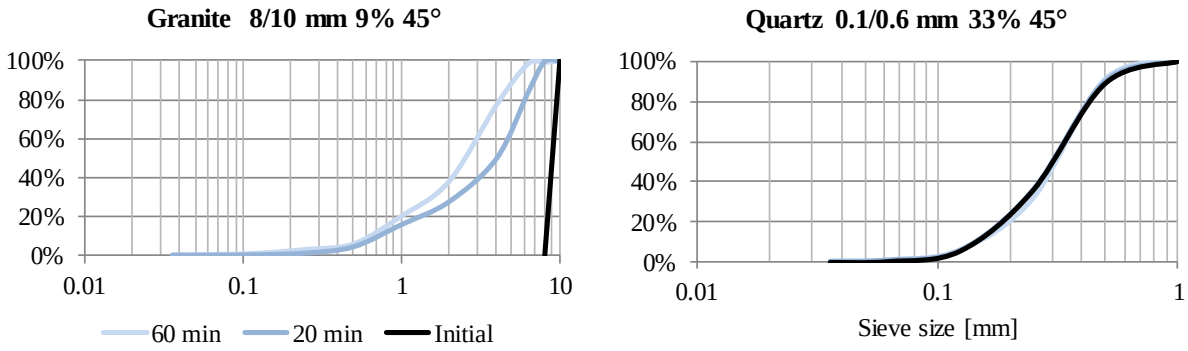

Figure 5: *Cumulative sieving results for both granite and quartz abrasives.*

Figure 6: *Tested 500HB steel sample with unused (upper row) and used (lower row) granite (left) and quartz (right) abrasives. The protected smooth edge areas are clearly visible on the sample surface.*

3.2. Characterization of wear surfaces

After the tests, the wear surfaces were first analyzed with an optical 3D-profilometer to get an overall picture of the extent of wear. The actual wear mechanisms were examined at higher magnifications using the profilometer for the elastomers and SEM for the steels. In all samples, wear initially concentrated on the upper corner area of the outer edge and then progressed to cover the whole sample area. The wear rate was visibly highest on the outer edge of the samples, where the peripheral speed is also the highest. The steels showed plastic deformation on the macroscopic level, which on the microscopic level eventually led to cracking and brittle detachment of the deformed surface layers. In addition, the elastomers showed plastic type of deformation, but the main material removal mechanisms typical to this type of materials were cutting and tearing off.

Fig. 7 presents the effect of test time on the 500HB steel, showing that the wear surfaces of both samples are quite similar. The SEM images were taken with the backscatter electron detector (BSE), which shows the steel in a lighter gray color while the abrasives appear dark. It should be noted that the magnification is different for granite in Figs. 7a-b and quartz in Figs. 7c-d. The much larger granite leaves wide and long scratches and large bits of fractured mineral on the surface, when plastically ploughing the material. With fine quartz, the scratches are only a few micrometers wide and barely visible. With granite, the wear surfaces of the steels were also slightly cleaned from excess embedded rock when the test time increased, while with the finer quartz abrasives the embedment of particles increased slightly throughout the tests.

In contrast to the steels, the elastomers showed increasing embedment of both abrasives with increasing test time. Over the whole wear surfaces, the embedment of fine quartz was higher than that of large granite, especially for the natural rubber. For both elastomers, fine quartz produced a rather smooth surface, while large granite caused grooves and pits with various depths on the surfaces, as presented in Fig. 8. The figure also shows the difference in the embedment between the abrasives: while large granite was comminuted during the test and then embedded as tiny pieces (Fig. 8a), the quartz particles were embedded also as larger particles (Fig. 8b).

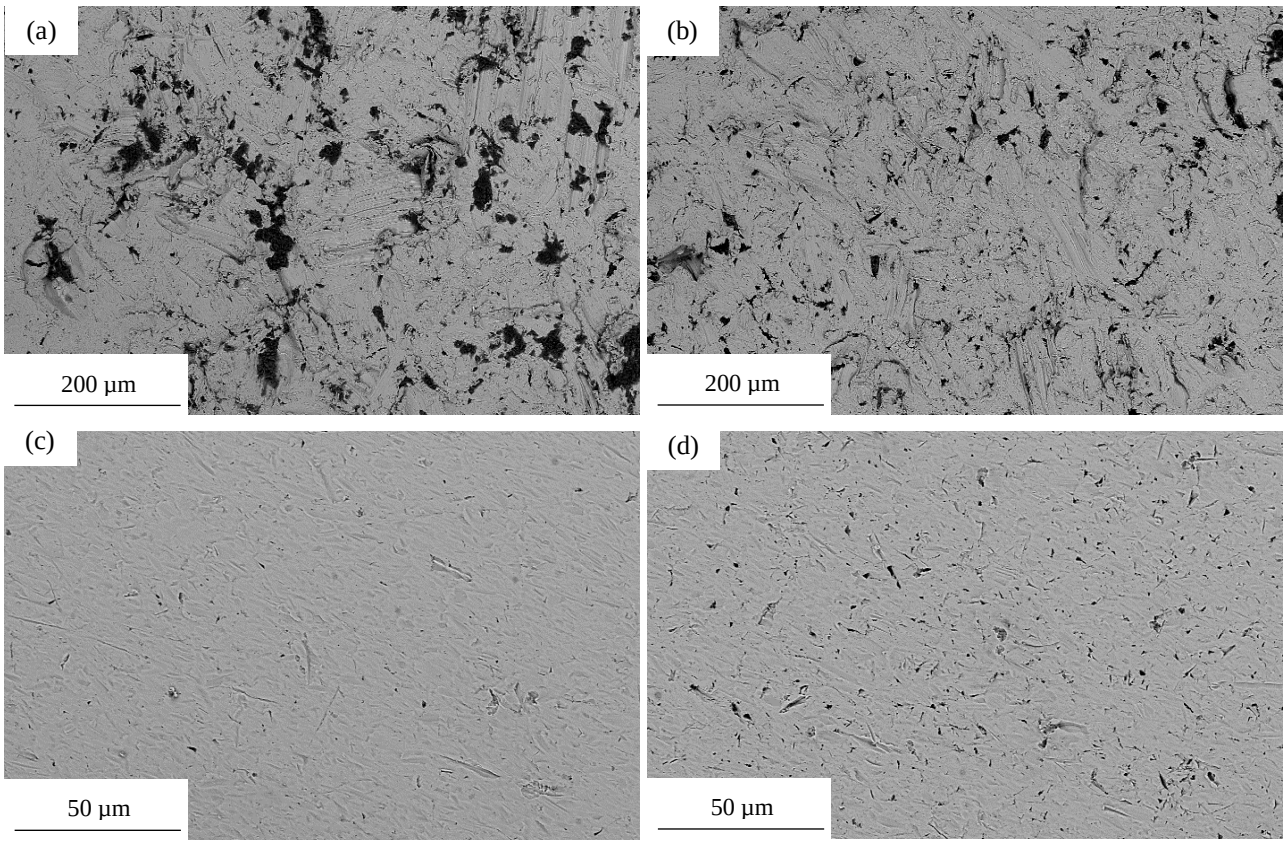

Figure 7: *BSE SEM images of the wear surfaces, revealing the amount of embedded abrasives on the 500HB steel after a) 20 minutes and b) 80 minutes of testing with the granite slurry, and corresponding images c) and d) after tests with the quartz slurry (note the different magnifications).*

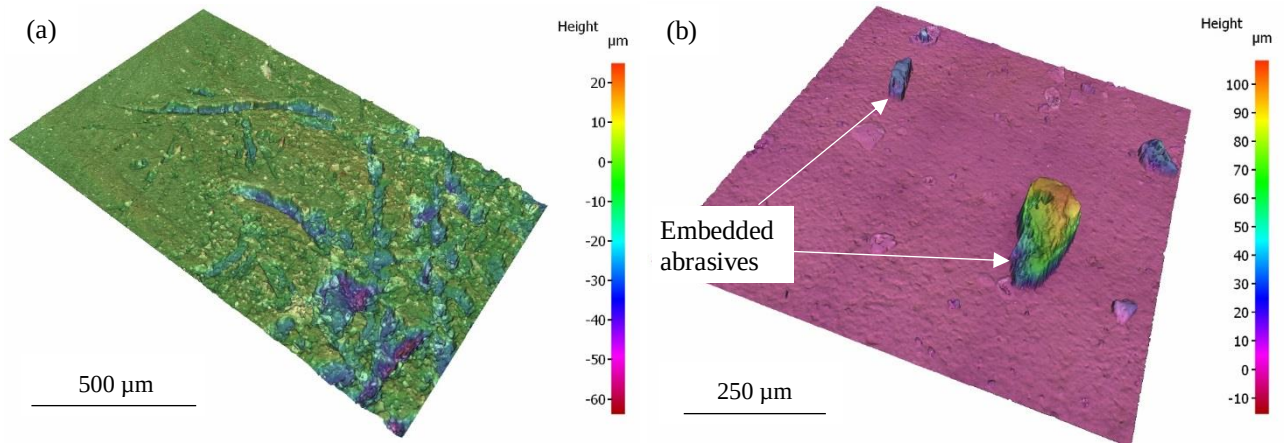

Figure 8: *3D profilometer images of elastomer wear surfaces after 80 minutes of testing, a) PU tested with granite and b) NR tested with quartz slurry. Note the different scales.*

For the studied materials, the wear marks intensified with increasing test time. Fig. 9 presents single particle impacts on a 500HB steel sample observed after 20 and 80 minutes of testing with granite slurry. After 20 minutes, there are still also rather smooth areas on the surface around the impact points, but after 80 minutes such areas could not be found anymore. For steels, the single impact marks were mostly similar regardless of

the test time, with a cut zone behind and a plastically deformed plough zone in front of the marks. The number of embedded granite abrasives on the surfaces of the steel samples in the form of broken tips of larger particles colliding on the surface was smaller and their separation larger compared with the elastomer surfaces. Furthermore, the abrasive remnants on the steel surfaces were typically larger than on the elastomer surfaces, where large pieces of granite abrasives were generally not found.

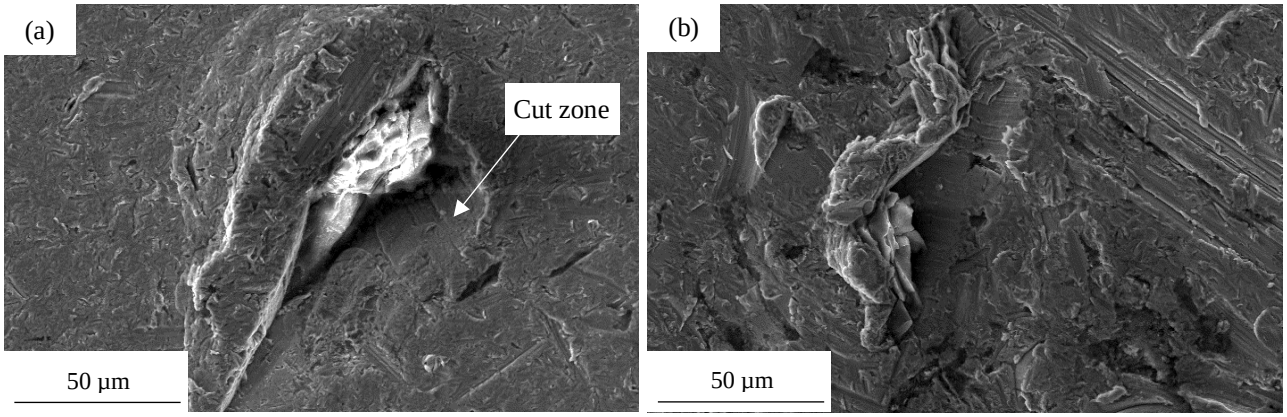

Figure 9: *Single impacts by granite particles on the 500HB steel after a) 20 minutes and b) 80 minutes of testing.*

The longest scratches were found in the 500HB steel. In addition, polyurethane contained long continuous wear marks, which most likely are not single scratches but coalesced pits of removed material, such as seen in Fig. 8. In any case, for both materials the longest scratches were around 500 µm long and observed in the tests with granite slurry.

Plastic deformation of the steels varied from fine cuttings by tiny quartz particles to massive ploughings by large granite particles. Fig. 10 shows an example of the latter for the 400HB steel. Similar 200-400 µm wide lip formations were observed in both steels. Plastic deformation leads to work hardening, and the abundantly deformed surface areas exhibited already some brittle features, such as cracks and detachment of lip edges by microfatigue (Fig. 10b). Furthermore, lip formation in high-stress wear always involves also mixing of the steel and abrasive materials. This often leads to a situation where a highly deformed and hardened lip is separated from the steel surface by embedded abrasives or a steel-abrasive composite layer.

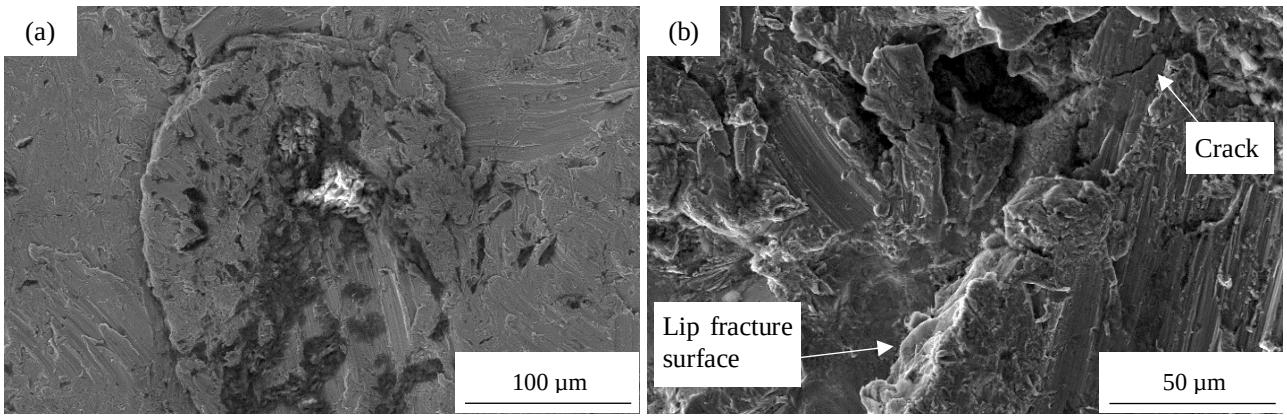

Figure 10: *Massive ploughing in the 400HB steel a) after 20 minutes of testing with granite slurry, leading to b) local cracking after 80 minutes of testing.*

3.3. Wear surface cross-sections

Wear surface cross-sections were prepared from the steel samples for more detailed evaluation of the wear behavior. With the edge protected samples, no clear white layers were found on the wear surfaces, but the 500HB steel contained some near surface shear bands. In a similar manner as in the previous study without edge protection, the fine quartz slurry did not produce any notable deformation in the samples. With large granite slurry, in general, the softer of the steels experienced more plastic deformation in terms of deformation depth, while the harder of the steels contained more thin layers with intense deformation approaching the white layer formation. Average deformation depths were 5 – 30 µm and 5 – 10 µm for the 400HB and 500HB steels, respectively.

Fig. 11 presents examples of the surface deformation of both steels tested with granite slurry. In the 400HB steel, 10 – 50 µm deep pits with strongly deformed surface can be observed. These deformation zones are smoothly oriented without any sharp transitions from the base material. On the other hand, in the 500HB steel the pits were shallower and the deformation zones less smooth and also notably thinner. Fig. 11 also shows a near surface shear band in the 500HB steel and a lip pushed on top of it with abrasive remnants between the two. Furthermore, there is a sharp cut through the shear band. Similar cuts were found in the same steel also in the previous study. The microhardness measurements showed that the surface of the 400HB steel was hardened slightly more than that of the 500HB steel, the average near surface hardness being 610 HV50gf and 690 HV50gf, respectively. The corresponding bulk hardness values of the steels were 480 HV50gf and 595 HV50gf. The highest measured hardness values obtained from the intense surface deformation areas were up to 700 HV50gf.

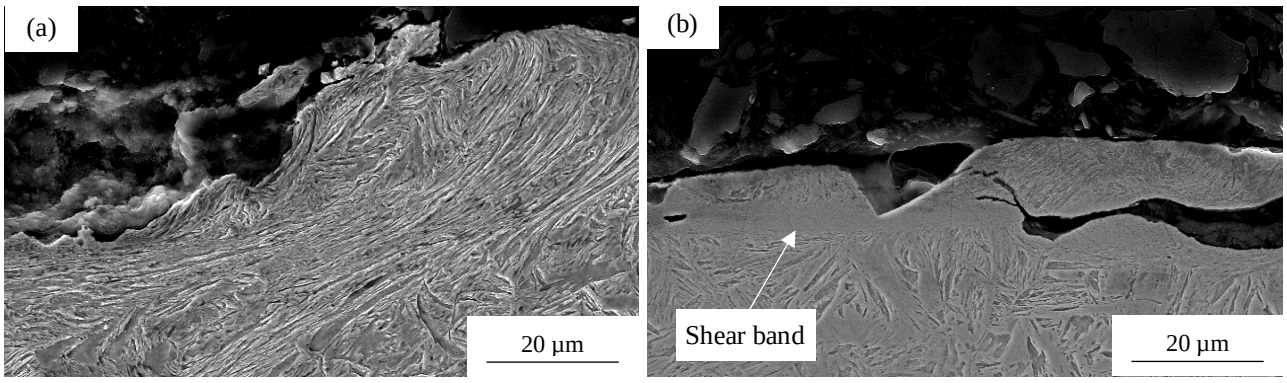

Figure 11: *Wear surface deformation on a) 400HB and b) 500HB steels after 80 minutes of testing with granite slurry.*

In contrast to granite, quartz did not produce observable deformations in either of the steels, as can be seen in Fig. 12. On the surface of the softer steel, cutting of the topmost layer was observed in a few cases. The harder steel had an almost perfectly flat and smooth surface after the tests, and only some sporadic a few microns deep holes or embedded pieces of abrasives were found. A thin abrasive layer covering most of the surface of both steels was also observed. For the 400HB steel the abrasive layer was about twice as thick. For the samples tested with fine quartz slurry, the microhardness measurements did not show any work hardening.

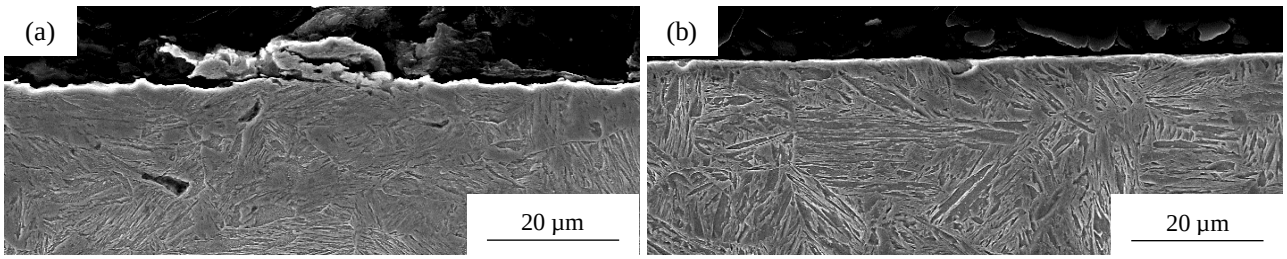

Figure 12: *Deformation of the wear surface of a) 400HB and b) 500HB steel samples after 80 minutes with quartz slurry.*

3.4. Particle embedment

To analyze the possible errors in the volume loss calculations caused by particle embedment, 3D-profilometry was experimented as a direct method to measure the volume losses. The samples where measured as they were, i.e. without the support of the edge protection window. For the rigid steel samples the measurement was a fairly simple task, but for the flexible elastomers it was difficult or even impossible. Some of the elastomer samples were so curved that it was impossible to get any reliable data. As it was not possible to get data from all samples, these measurements are used only as a suggestive data. Nevertheless, X-ray measurements done for the elastomers in the previous study and the cross-section studies done for the steels have indicated a clear difference in the particle embedment behavior between the material types.

Fig. 13 presents profilometer images for the 400HB steel and the NR elastomer tested with the granite slurry at +45° sample angle for 80 minutes. Especially for the elastomers, the profilometer studies were more reliable after longer test times. As seen in Figure 13, for the steels the direct volume loss measurement is rather straightforward, but for the elastomers some extra work needed to be done: in the volume measurement of the

NR sample, the cutting marks on the left hand side and in the right side corners, as well as the 'valley' at the bottom, were excluded. Table 3 presents the comparison between the wear loss results obtained by weighing and by the use of the profilometer.

Table 3: Comparison of wear loss determinations after 80 minutes of testing with granite slurry for 400HB and NR.

	Volume loss calculated from mass loss [cm^3]	Direct volume loss measurement [cm^3]	Difference
400HB	0.027	0.020	-27 %
NR	0.015	0.025	+66 %

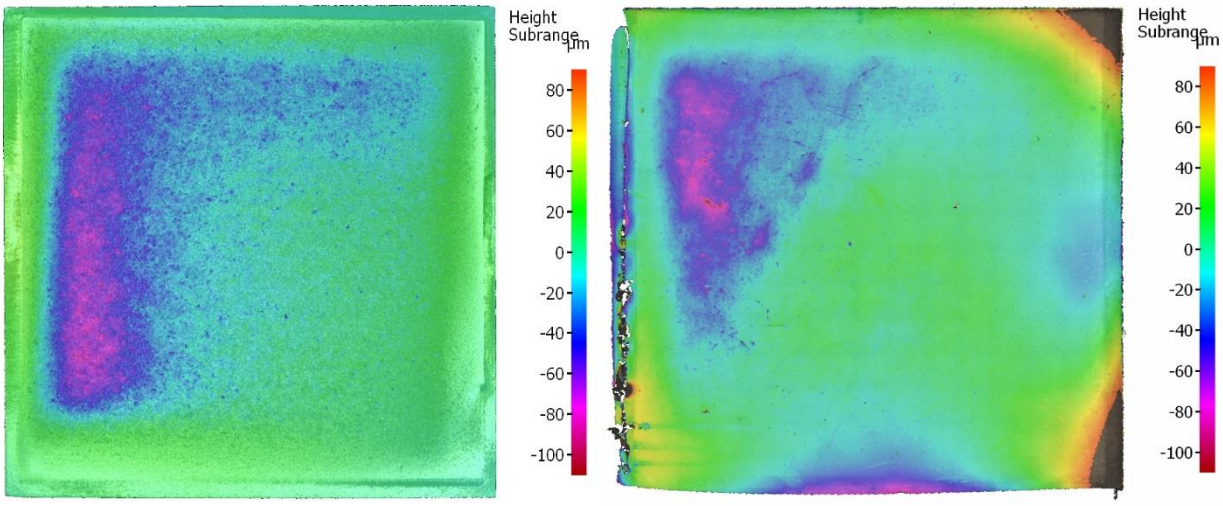

Figure 13: *Combined topography and texture images of 400HB and NR samples after 80 minutes of testing with granite slurry at +45° sample angle.*

4. DISCUSSION

In industrial slurry applications, the flow of slurry is often turbulent, which leads to random and varying impact angles of the abrasive particles [19,22,44]. Such erosion wear environment, for example in slurry transport, is highly complex and in practice often only partly controllable [45]. For the experimental simulation of such conditions, the high speed slurry-pot wear tester was used in this study. The tests were done with edge protected samples using large sized, 8/10 mm, and fine sized, 0.1/0.6 mm, abrasives. On one hand, the aim of this study was to investigate the material performance without edge wear, and on the hand to evaluate the edge effect on wear and to further study the particle embedment effect. In this chapter, the results of the current work with edge protected samples are discussed and compared to a previous study [6] conducted without edge protection.

To properly compare the wear performance of steels and elastomers, more than just wear loss data is needed. One such piece of information is the embedment of abrasives on the wear surface. Embedment of the abrasives in elastomeric materials has been noticed to take place during erosion, affecting also the measured wear loss

values [46,47]. In the previous study [6], the embedment was evaluated by X-ray diffraction, which showed that the surface layer of elastomeric materials tends to become filled with abrasives, while the surfaces of steels may even start to clean up over time, especially when larger particles are used. Moreover, the embedment, especially with fine particles, is much stronger with the elastomers than with the steels, i.e., the elastomers contain higher amounts of abrasive material stuck on their surfaces than the steels.

The embedment affects the determined mass loss values and the relative wear performance ranking, especially as the embedded materials with densities of about 2.5 g/cm^3 are heavier than the elastomers but lighter than the steels. This means that even with the same amount of embedded particles, the embedment would make the elastomer look considerably less worn when the volume losses are calculated from the mass losses. By assuming the particles to be round with 100 µm average particle size and 4 % surface coverage, resulting in about 5000 embedded particles for the current specimen size, the embedment effect for the volume loss calculated from the mass losses would be +2 % for steels but +130 % for the elastomers. Based on the direct volume loss measurements done with the 3D-profilometer, the calculated volume losses for the elastomers are on average about 30 – 40 % too low, being largest with fine quartz and lowest with large granite. This is supported by the visual observations of embedding being higher with the use of smaller particles. For the steels, the difference between the determined volume losses were opposite, i.e. 10 – 30 % too high when determined based on the weighing results.

Another important factor in the case of batch operated wear tests is the comminution of the abrasives. When the duration of individual tests is increased, the degree of comminution will become higher and the wear environment will contain more and more crushed smaller particles. In the current tests with large granite this would lead to a condition where the amount of fine quartzite particles increases, as quartzite is the hardest phase of granite. With decreasing abrasive size, the work hardening of steels will decrease and the particle embedment in elastomers will increase. This means that the effect of comminution on the wear rate is different for the different types of materials.

By comparing the current results with the ones obtained from the previous study [6], the edge effect in slurry erosion can be evaluated. The steels received the same mutual ranking in both tests, whereas the ranking order of the elastomers was reversed. With edge wear the natural rubber was always better than the polyurethane, but with edge protection the polyurethane was better in three cases out of six, when the test parameters were varied. Fig. 14 presents a comparison between the two studies. As the sample sizes were not identical, the results have been normalized by the true wear area in a similar manner as in the study by Ratia et al. [28].

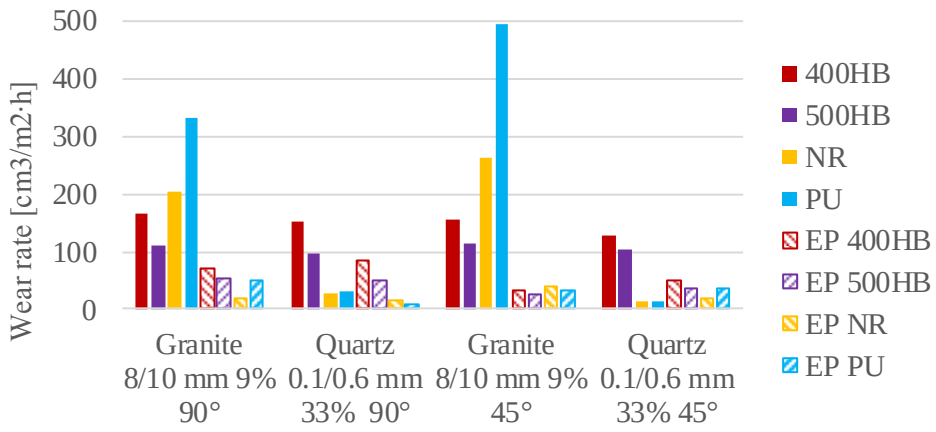

Figure 14: *Comparison of the wear rates of plate samples with (EP) and without edge protection.*

The sample angles of 45° and 90° were used both in the tests with and without edge protection. In the previous tests without edge protection, the sample angle did not have any notable effect on the obtained results. With edge protection, however, significant differences were observed: 53 – 117 % for the steels with the lower angle causing less material loss, and 2 – 120 % for the elastomers with the higher angle causing less materials loss. The different effect of the nominal impact angle is in agreement with the general erosion theories, i.e., wear resistant steels, not being distinctly ductile nor brittle, perform in general better at lower angles while elastomers perform better at higher angles [48,49]. For all tested materials, the biggest edge effect was observed with large granite particles and 45° sample angle. A similar abrasive size effect was noticed in the earlier study in dry high-stress abrasion conditions [27]. Furthermore, on average the elastomers suffered from a bigger edge effect with all test parameters, except for fine quartz at the 45° sample angle. Table 4 presents the edge effect for each test parameter and test material as the ratio of the bars shown in Fig. 14.

Table 4: *Edge effect as the wear rate ratio between unprotected and (edge) protected samples.*

	Granite 8/10 mm 9% 90°	Quartz 0.1/0.6 mm 33% 90°	Granite 8/10 mm 9% 45°	Quartz 0.1/0.6 mm 33% 45°
400HB	2.4	1.8	5.0	2.5
500HB	2.1	2.0	4.5	2.9
NR	10.1	1.7	6.4	0.8
PU	6.7	3.4	16.0	0.4

The comparison of the results with and without edge protection shows that all test materials have a significantly lower wear rate in most of the conditions, when the sample edges are protected. This is not as such surprising, but it should also be noted that the changes are different for the steels and elastomers. The steels behave in a more consistent manner, whereas the elastomers show much bigger differences and even a negative edge effect with fine quartz at 45° sample angle, i.e., higher wear rates when the edges are protected. There are two possible explanations for that: 1) without edge protection the edge areas of the elastic material can bend rather freely in the slurry flow, while with edge protection the deformation of the sample is more constrained, and 2) without

edge protection the effective area of the sample is more than twice that of the protected sample, which means that higher particle embedment can rise the mass of the sample relatively more than with the protected sample.

5. CONCLUSIONS

In this study, high speed slurry erosion tests were conducted with edge protected samples for evaluating the edge effect in the abrasive wear behavior of wear resistant steels and elastomers. The results of similar tests conducted without edge protection were used as reference data [6]. The test materials were two wear resistant steels with hardness grades of 400 and 500 HB, and two elastomers, a natural rubber and a polyurethane, which are used for example as lining materials in slurry applications. The test program included both high-stress and low-stress conditions, achieved by two different abrasives. The main findings of the study are as follows:

- The larger the abrasive, the higher the material loss it inflicts on the sample. Furthermore, the edge wear is also more dominant with larger abrasives. However, the difference between the steel grades was largest with fine abrasives. This is due to the minute work hardening effect caused by the fine quartz particles, as observed in both studies.
- On average, the elastomers showed twice as large edge effect as the steels.
- While the ranking and differences between the steels were more or less consistent with all test parameters, the same was not true with the elastomers. For them, the mutual ranking varied depending on the test parameters, i.e., the wear environment.
- The wear mechanisms were essentially the same in both edge protected and unprotected tests. On the steel surfaces, the large granite slurry produced abrasive scratches and impact marks by repeated and continuous impacts of the particles, while the elastomers suffered mostly from cutting and tearing. The fine quartz slurry caused mainly low-stress cutting on both material types.
- A huge difference was noticed in the embedment of the abrasives. Especially with fine quartz, the embedment of abrasives in the elastomers was extensive. With 3D-profilometry, the effect of particle embedment on the wear performance was observed to be notable.
- The main difference between the two studied steels was in the extent of wear surface deformation. With large particles, the 400HB steel showed much higher deformation depths and also more smoothly oriented deformed zones than the 500HB steel.
- The initially softer steel also work hardened more than the harder one, as both steels ended up at a more or less same peak hardness of the deformed wear surface.

ACKNOWLEDGEMENTS

The work has been done within the DIMECC BSA (Breakthrough Steels and Applications) programme as part of the DIMECC Breakthrough Materials Doctoral School. We gratefully acknowledge the financial support from the Finnish Funding Agency for Innovation (Tekes) and the participating companies. The authors also gratefully acknowledge Specialist Anu Kemppainen from SSAB Europe Oy for her help and advices. The corresponding author would like to express his gratitude to Jenny and Antti Wihuri Foundation, and Finnish Cultural Foundation.

REFERENCES

[1] T. Da Silva, Interview - Slurry Pipelines: Exciting Technology Entering Period of Renaissance, (2012). http://ceo.ca/2012/10/10/slurry-pipelines-exciting-technology-entering-period-of-renaissance/ (accessed December 12, 2015).

[2] L.L. Parent, D.Y. Li, Wear of hydrotransport lines in Athabasca oil sands, Wear. 301 (2013) 477–482. doi:10.1016/j.wear.2013.01.039.

[3] Basics in Minerals Processing, 6th ed., Metso Minerals, Inc., 2008.

[4] C.I. Walker, P. Robbie, Comparison of some laboratory wear tests and field wear in slurry pumps, Wear. 302 (2013) 1026–1034. doi:10.1016/j.wear.2012.11.053.

[5] N. Ojala, K. Valtonen, P. Kivikytö-reponen, P. Vuorinen, V. Kuokkala, High speed slurry-pot erosion wear testing with large abrasive particles, Finnish J. Tribol. (2015).

[6] N. Ojala, K. Valtonen, A. Kemppainen, J. Minkkinen, O. Oja, V. Kuokkala, Wear performance of quenched wear resistant steels in abrasive slurry erosion, Wear. (2016).

[7] A.A. Gadhikar, A. Sharma, D.B. Goel, C.P. Sharma, Fabrication and Testing of Slurry Pot Erosion Tester, Trans. Indian Inst. Met. 64 (2011) 493–500. doi:10.1007/s12666-011-0075-8.

[8] G.R. Desale, B.K. Gandhi, S.C. Jain, Improvement in the design of a pot tester to simulate erosion wear due to solid–liquid mixture, Wear. 259 (2005) 196–202. doi:10.1016/j.wear.2005.02.068.

[9] H.M. Clark, R.B. Hartwich, A re-examination of the "particle size effect" in slurry erosion, Wear. 248 (2001) 147–161. doi:10.1016/S0043-1648(00)00556-1.

[10] A. Jankovic, Variables affecting the fine grinding of minerals using stirred mills, Miner. Eng. 16 (2003) 337–345. doi:10.1016/S0892-6875(03)00007-4.

[11] N. Ojala, K. Valtonen, P. Kivikytö-Reponen, P. Vuorinen, P. Siitonen, V.-T. Kuokkala, Effect of test parameters on large particle high speed slurry erosion testing, Tribol. - Mater. Surfaces Interfaces. 8 (2014) 98–104. doi:10.1179/1751584X14Y.0000000066.

[12] P.D. Jakobsen, L. Langmaack, F. Dahl, T. Breivik, Development of the Soft Ground Abrasion Tester (SGAT) to predict TBM tool wear, torque and thrust, Tunn. Undergr. Sp. Technol. 38 (2013) 398–408. doi:10.1016/j.tust.2013.07.021.

[13] V. Levonmaa, Interview on 17.2.2014, (2014) Aquamec Oy, Finland.

[14] H.M. Clark, R.J. Llewellyn, Assessment of the erosion resistance of steels used for slurry handling and transport in mineral processing applications, Wear. 250 (2001) 32–44. doi:10.1016/S0043-1648(01)00628-7.

[15] N. Pereira Abbade, S. João Crnkovic, Sand–water slurry erosion of API 5L X65 pipe steel as quenched from intercritical temperature, Tribol. Int. 33 (2000) 811–816. doi:10.1016/S0301-679X(00)00126-2.

[16] Y.I. Oka, H. Ohnogi, T. Hosokawa, M. Matsumura, The impact angle dependence of erosion damage caused by solid particle impact, Wear. 203–204 (1997) 573–579. doi:10.1016/S0043-1648(96)07430-3.

[17] R. Suihkonen, J. Perolainen, M. Lindgren, K. Valtonen, N. Ojala, E. Sarlin, et al., Erosion wear of glass fibre reinforced vinyl ester, Tribol. - Finnish J. Tribol. 33 (2015) 11–19.

[18] B.W. Madsen, A comparison of the wear of polymers and metal alloys in laboratory and field slurries, Wear. 134 (1989) 59–79. doi:10.1016/0043-1648(89)90062-8.

[19] Y. Xie, J. (Jimmy) Jiang, K.Y. Tufa, S. Yick, Wear resistance of materials used for slurry transport, Wear. 332–333 (2015) 1104–1110. doi:10.1016/j.wear.2015.01.005.

[20] B.T. Lu, J.F. Lu, J.L. Luo, Erosion–corrosion of carbon steel in simulated tailing slurries, Corros. Sci. 53 (2011) 1000–1008. doi:10.1016/j.corsci.2010.11.034.

[21] Y. Yang, Y.F. Cheng, Parametric effects on the erosion–corrosion rate and mechanism of carbon steel pipes in oil sands slurry, Wear. 276–277 (2012) 141–148. doi:10.1016/j.wear.2011.12.010.

[22] M.. Stack, N. Corlett, S. Turgoose, Some thoughts on modelling the effects of oxygen and particle concentration on the erosion–corrosion of steels in aqueous slurries, Wear. 255 (2003) 225–236. doi:10.1016/S0043-1648(03)00205-9.

[23] R. Gupta, S.N. Singh, V. Sehadri, Prediction of uneven wear in a slurry pipeline on the basis of measurements in a pot tester, Wear. 184 (1995) 169–178. doi:10.1016/0043-1648(94)06566-7.

[24] G.R. Desale, B.K. Gandhi, S.C. Jain, Effect of erodent properties on erosion wear of ductile type materials, Wear. 261 (2006) 914–921. doi:10.1016/j.wear.2006.01.035.

[25] A. Neville, C. Wang, Erosion–corrosion of engineering steels—Can it be managed by use of chemicals?, Wear. 267 (2009) 2018–2026. doi:10.1016/j.wear.2009.06.041.

[26] R. Suihkonen, J. Perolainen, M. Lindgren, K. Valtonen, N. Ojala, E. Sarlin, et al., Erosion wear of glass fibre reinforced vinyl ester, in: 16th Nord. Symp. Tribol. - Nord. 2014, Aarhus, 2014: pp. 1–6.

[27] J. Terva, V. Kuokkala, P. Kivikytö-reponen, The edge effect of specimens in abrasive wear testing, Finnish J. Tribol. 31 (2012) 27–35.

[28] V. Ratia, K. Valtonen, A. Kemppainen, V. Kuokkala, The Role of Edge-Concentrated Wear in Impact-Abrasion Testing, Tribol. Online. (2015).

[29] I.M. Hutchings, Deformation of metal surfaces by the oblique impact of square plates, Int. J. Mech. Sci. 19 (1977) 45–52. doi:10.1016/0020-7403(77)90015-7.

[30] S. Yerramareddy, S. Bahadur, Effect of operational variables, microstructure and mechanical properties on the erosion of Ti-6Al-4V, Wear. 142 (1991) 253–263. doi:10.1016/0043-1648(91)90168-T.

[31] S.M. Walley, J.E. Field, The Erosion and Deformation of Polyethylene by Solid-Particle Impact, Philos. Trans. R. Soc. A Math. Phys. Eng. Sci. 321 (1987) 277–303. doi:10.1098/rsta.1987.0016.

[32] S. Lathabai, M. Ottmüller, I. Fernandez, Solid particle erosion behaviour of thermal sprayed ceramic, metallic and polymer coatings, Wear. 221 (1998) 93–108. doi:10.1016/S0043-1648(98)00267-1.

[33] J.B. Zu, G.T. Burstein, I.M. Hutchings, A comparative study of the slurry erosion and free-fall particle erosion of aluminium, Wear. 149 (1991) 73–84. doi:10.1016/0043-1648(91)90365-2.

[34] L. Chen, G. Luo, K. Liu, J. Ma, B. Yao, Y. Yan, et al., Bonding of glass-based microfluidic chips at low- or room-temperature in routine laboratory, Sensors Actuators B Chem. 119 (2006) 335–344.

doi:10.1016/j.snb.2005.11.052.

[35] W. Wu, K.C. Goretta, J.L. Routbort, Erosion of 2014 Al reinforced with SiC or Al2O3 particles, Mater. Sci. Eng. A. 151 (1992) 85–95. doi:10.1016/0921-5093(92)90185-4.

[36] M. Papini, J.K. Spelt, Impact of rigid angular particles with fully-plastic targets Part II: Parametric study of erosion phenomena, Int. J. Mech. Sci. 42 (2000) 1007–1025. doi:10.1016/S0020-7403(99)00024-7.

[37] H. Getu, J.K. Spelt, M. Papini, Reduction of particle embedding in solid particle erosion of polymers, Wear. 270 (2011) 922–928. doi:10.1016/j.wear.2011.02.012.

[38] H. Getu, J.K. Spelt, M. Papini, Conditions leading to the embedding of angular and spherical particles during the solid particle erosion of polymers, Wear. 292 (2012) 159–168. doi:10.1016/j.wear.2012.05.017.

[39] V. Hadavi, B. Michaelsen, M. Papini, Measurements and modeling of instantaneous particle orientation within abrasive air jets and implications for particle embedding, Wear. 336 (2015) 9–20. doi:10.1016/j.wear.2015.04.016.

[40] V. Hadavi, M. Papini, Numerical modeling of particle embedment during solid particle erosion of ductile materials, Wear. 342 (2015) 310–321. doi:10.1016/j.wear.2015.09.008.

[41] P. Kulu, R. Veinthal, M. Saarna, R. Tarbe, Surface fatigue processes at impact wear of powder materials, Wear. 263 (2007) 463–471. doi:10.1016/j.wear.2006.11.033.

[42] B. Yu, D.Y. Li, A. Grondin, Effects of the dissolved oxygen and slurry velocity on erosion–corrosion of carbon steel in aqueous slurries with carbon dioxide and silica sand, Wear. 302 (2013) 1609–1614. doi:10.1016/j.wear.2013.01.044.

[43] V. Ratia, V. Heino, K. Valtonen, M. Vippola, A. Kemppainen, P. Siitonen, et al., Effect of abrasive properties on the high-stress three-body abrasion of steels and hard metals, Tribol. - Finnish J. Tribol. 32 (2014) 3–18.

[44] A.J.C. Paterson, High density slurry and paste tailings, transport systems, in: Int. Platin. Conf. Platin. Adding Value, 2004: pp. 159–166. http://www.hydrometallurgy.co.za/Pt2004/Papers/159_Paterson.pdf.

[45] G.F. Truscott, Wear in pumps and pipelines, Wear Slurry Pipelines - BHRA Inf. Ser. 1 (1980).

[46] N.M. Barkoula, J. Karger-Kocsis, Processes and influencing parameters of the solid particle erosion of polymers and their composites, J. Mater. Sci. 37 (2002) 3807–3820. doi:10.1023/A:1019633515481.

[47] G.W. Stachowiak, A.W. Batchelor, Abrasive, Erosive and Cavitation wear, in: Eng. Tribol., 4th editio, Elsevier, 2014: pp. 525–576. doi:10.1016/B978-0-12-397047-3.00011-4.

[48] K.-H. Zum Gahr, Microstructure and Wear of Materials, Elsevier, Amsterdam, 1987. doi:10.1016/S0167-8922(08)70719-3.

[49] E. Huttunen-Saarivirta, H. Kinnunen, J. Tuiremo, M. Uusitalo, M. Antonov, Erosive wear of boiler steels by sand and ash, Wear. 317 (2014) 213–224. doi:10.1016/j.wear.2014.06.007.